Synthesis and Optical Properties of Conjugated Polymers Containing Polyoxometalate Clusters as Side-Chain Pendants

Bubin Xu, Meng Lu, Jeonghee Kang, Degang Wang, John Brown, and Zhonghua Peng*

Department of Chemistry, University of Missouri−Kansas City, Kansas City, Missouri 64110

Received January 26, 2005. Revised Manuscript Received March 22, 2005

Hexamolybdate clusters have been covalently attached, for the first time, to the side chains of conjugated polymers. Two sets of such hybrid conjugated polymers have been prepared, one (**Ia** and **Ib**) with the clusters linked to the conjugated backbone through a rigid conjugated bridge, the other (**IIa** and **IIb**) through flexible alkyl chains. Within each set, polymers with different cluster loading ratios have been prepared. The covalent attachment of POM clusters has been confirmed by ^{1}H NMR, FTIR, and cyclic voltammetry measurements. These hybrid polymers are thermally stable up to 220 °C. Set **I** polymers (**Ia** and **Ib**) exhibit maximum absorption wavelengths (λ_{max}) around 410 nm, while set **II** polymers (**IIa** and **IIb**) show higher λ_{max} values, around 440 nm. Fluorescence studies show that side-chain POM pendants linked through conjugated bridges exhibit a much higher fluorescence quenching effect than those with flexible alkyl bridges, indicating that the through-bond photoinduced electron transfer may be the dominant mechanism for fluorescence quenching. With efficient fluorescence quenching that results in free charge carriers residing in different structural units (positively charged holes in the PPE backbone and negatively charged electrons in the POM clusters), these hybrid polymers may have great potential for applications in photovoltaic (PV) cells.

Introduction

Conjugated polymers are perhaps the most widely and extensively studied systems in the past decades.[1] Fueling the heat are a series of exciting discoveries including the demonstrations of polymer light-emitting diodes,[2] polymer-based transistors,[3] ultra-sensitive sensory systems,[4] and polymer photovoltaic (PV) cells,[5] etc. leading to a whole new research arena of plastic electronics. One unique feature for conjugated polymers is the great flexibility in anchoring additional functional units to their side chains, allowing not only the fine-tuning of their electronic/optical properties but also the realization of new properties resulting from synergistic effects.[1] For example, anchoring nonlinear optical chromophores to a conjugated polymer backbone has led to photorefractive materials,[6] and introducing chemically persistent pendant radicals may result in organic molecular or nanomagnets.[7] Linking electron acceptors, such as C^{60} to conjugated polymers as side-chain pendants has resulted in systems with highly efficient photoinduced electron transfer, which has led to the fabrication of efficient solar cells.[8] Polyoxometalates (POMs) are attractive molecular clusters not only because of their unlimited structural versatilities and appealing structural features[9] but also due to their rich electrical and optical properties,[10] one of which is indeed their electron-accepting capability. The reduction process is usually reversible and occurs with marginal structural variations. It is envisioned that a hybrid conjugated polymer with POM clusters as side-chain pendants may exhibit efficient photoinduced electron transfer from the polymer backbone to the POM cluster.[11] With free charge carriers residing in different structural units, charge recombination may be minimized. We recently reported main-chain POM-contain-

* Corresponding author. Phone: (816) 235-2288; fax: (816) 235-5502; e-mail: pengz@umkc.edu.

(1) (a) *Handbook of Organic Conductive Molecules and Polymers*, Vols. I−IV; Nalwa, H. S., Ed.; John Wiley & Sons: Chichester, England, 1997. (b) *Conjugated Polymers*; Bredas, J. L., Silbey, R., Eds.; Kluwer Academic Publishers: Dordrecht, The Netherlands, 1991. (c) *Handbook of Conducting Polymers*, 2nd ed.; Skotheim, T. A., Elsenbaumer, R. L., Reynolds, J. R., Eds.; Marcel Dekker: New York, 1998.

(2) (a) Burroughes, J. H.; Bradley, D. D. C.; Brown, A. R.; Marks, R. N.; Mackay, K.; Friend, R. H.; Burn, P. L.; Holmes, A. B. *Nature* **1990**, *347*, 539. (b) Gustafsson, G.; Cao, Y.; Treacy, G. M.; Klavetter, F.; Colaneri, N.; Heeger, A. J. *Nature* **1992**, *357*, 477. (c) Kraft, A.; Grimsdale, A. C.; Holmes, A. B. *Angew. Chem., Int. Ed. Eng.* **1998**, *37*, 402.

(3) (a) Shirringhaus, H.; Tessler, N.; Friend, R. H. *Science* **1998**, *280*, 1741. (b) Dimitrakopoulos, C. D.; Malenfant, P. R. L. *Adv. Mater.* **2002**, *14*, 99. (c) Katz, H. E.; Bao, Z. *J. Phys. Chem. B* **2000**, *104*, 671. (d) Horowitz, G. *Adv. Mater.* **1998**, *10*, 365. (e) Babel, A.; Jenekhe, S. A. *J. Am. Chem. Soc.* **2003**, *125*, 13656.

(4) (a) Leclerc, M.; Faïd, K. *Adv. Mater.* **1997**, *9*, 1087. (b) McQuade, D. T.; Pullen, A. E.; Swager, T. M. *Chem. Rev.* **2000**, *100*, 2537. (c) Gaylord, B. S.; Heeger, A. J.; Bazan, G. C. *J. Am. Chem. Soc.* **2003**, *125*, 896.

(5) (a) Sariciftci, N. S.; Smilowitz, L.; Heeger, A. J.; Wudl, F. *Science* **1992**, *258*, 1474. (b) Sariciftci, N. S.; Braun, D.; Zhang, C.; Srdanov, V. I.; Heeger, A. J.; Stucky, G.; Wudl, F. *Appl. Phys. Lett.* **1993**, *62*, 585.

(6) Peng, Z.; Gharavi, A.; Yu, L. *J. Am. Chem. Soc.* **1997**, *119*, 4622.

(7) (a) Nishide, H.; Ozawa, T.; Miyasaka, M.; Tsuchida, E. *J. Am. Chem. Soc.* **2001**, *123*, 5942. (b) Nishide, H.; Miyasaka, M.; Doi, R.; Araki, T. *Macromolecules* **2002**, *35*, 690. (c) Murata, H.; Takahashi, M.; Namba, K.; Takahashi, N.; Nishide, H. *J. Org. Chem.* **2004**, *69*, 631.

(8) Ramos, A. M.; Rispens, M. T.; van Duren, J. K. J.; Hummelen, J. C.; Janssen, R. A. J. *J. Am. Chem. Soc.* **2001**, *123*, 6714.

(9) (a) *Heteropoly and Isopoly Oxometalates*; Pope, M. T., Ed.; Springer: New York, 1983. (b) *Polyoxometalates: From Platoic Solids to Anti-Retroviral Activity*; Pope, M. T., Müller, A., Eds.; Kluwer Academic: Dordrecht, The Netherlands, 1994. (c) Hill, C. L. *Chem. Rev.* **1998**, *98*, 8, No. 1.

(10) (a) Sadakane, M.; Steckhan, E. *Chem. Rev.* **1998**, *98*, 291. (b) Yamase, T. *Chem. Rev.* **1998**, *98*, 307. (c) Müller, A.; Shah, S. Q. N.; Bögge, H.; Schmidtmann, M.; Kögerler, P.; Hauptfleisch, B.; Leiding, S.; Wittler, K. *Angew. Chem., Int. Ed. Engl.* **2000**, *39*, 1614. (d) Coronado, E.; Gómez-García, C. J. *Chem. Rev.* **1998**, *98*, 273.

10.1021/cm050188r CCC: $30.25
Published on Web 05/03/2005

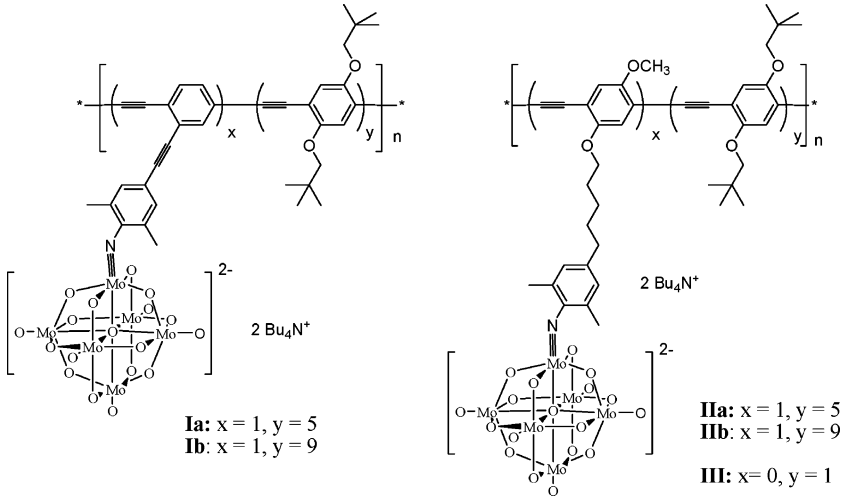

Figure 1. Structures of two sets of hybrid conjugated polymers and PP polymer **III**.

ing hybrid polymers that were shown to exhibit efficient photoinduced charge separation.[12] Their PV cell performance, albeit promising, is however limited by the poor charge-transporting properties of those polymers since they contain only limited π-extended conjugated segments. Conjugated polymers with POM as side-chain pendants are expected to be better candidates for PV applications as such polymers may exhibit both efficient charge separation and efficient charge transporting properties.[10d]

Hybrid materials based on organic conducting polymers and POM clusters have been the focus of research for over a decade.[13] The majority, if not all of the research, however, has been limited to composite materials where POM clusters are either embedded in a polymer matrix[14] or sandwiched between cationic polymers through layer-by-layer assembly.[15] Hybrid polymers with covalent attachment of POM clusters have so far been limited to insulating nonconjugated polymers.[16] In this paper, we report the detailed synthesis of the first two sets of hybrid conjugated polymers with POM clusters as side-chain pendants and the studies of their electronic, optical, and electrochemical properties.

Results and Discussion

Synthesis of Monomers and Polymers. Figure 1 shows the structures of the two sets of hybrid polymers. Both sets of polymers have a poly(phenylene ethynylene) (PPE) backbone, one of the most extensively studied conjugated polymer systems.[17] Hexamolybdate clusters are linked to the PPE backbone through either a rigid conjugated bridge (set **I** polymers) or a flexible non-π-conjugated alkyl bridge (set **II** polymers). It is so designed that the effect of π-conjugation on the photoinduced electron transfer from the PPE backbone to the POM cluster can be studied.

There are, in principle, two approaches to prepare the targeted polymer hybrids, namely, the polymerization−hybridization (polymerization first) approach and the hybridization−polymerization (hybridization first) approach. As shown in Scheme 1, the first route involves the synthesis of precursor polymers with arylamine functional pendants. The hybridization is then carried out on precursor polymers. The second approach starts with the synthesis of hybrid monomers, which are then used directly for the synthesis of the targeted polymers. While the first route may allow better control over the degree of polymerization and offers the convenience in synthesizing polymer hybrids with varying clusters, the post-polymerization−hybridization step lacks control on the extent of cluster functionalization. Furthermore, the four precursor polymers were found to exhibit rather poor solubility in organic solvents. We have thus chosen the second route, whose crucial step is the synthesis of hybrid monomers with two iodo or two ethynyl functional groups.

Scheme 2 shows the synthesis of a hybrid monomer where the cluster is anchored with a rigid organic π-system carrying remote bifunctionality (two ethynyl functional groups). 2-Iodio-1,4-dibromobenzene (**2**) was synthesized from 2,5-dibromoaniline through the Sandmeyer reaction. Taking advantage of the higher reactivity of iodo over bromo in the palladium-catalyzed Sonogashira coupling reactions,[18] the iodo group in **2** was selectively converted to an ethynyl group (compound **3**), which was then selectively coupled with

(11) (a) Liu, S.; Kurth, D. G.; Mohwald, H.; Volkmer, D. *Adv. Mater.* **2002**, *14*, 225. (b) Moriguchi, I.; Fendler, J. H. *Chem. Mater.* **1998**, *10*, 2205.
(12) Lu, M.; Xie, B.; Kang, J.; Chen, F.; Yang, Y.; Peng, Z. *Chem. Mater.* **2005**, *17*, 402.
(13) (a) Katsoulis, E. D. *Chem. Rev.* **1998**, *98*, 359. (b) Sanchez, C.; Soler-Illia, G. J. A. A.; Ribot, F.; Lalot, T.; Mayer, C. R.; Cabuil, V. *Chem. Mater.* **2001**, *13*, 3061.
(14) (a) Shimidzu, T.; Ohtani, A.; Aiba, M.; Honda, K. *J. Chem. Soc., Faraday Trans.* **1988**, *84*, 3941. (b) Bidan, G.; Geniès, E. M.; Lapkowski, M. *J. Chem. Soc., Chem. Commun.* **1988**, 533. (c) Fabre, B.; Bidan, G.; Laplowski, M. *J. Chem. Soc., Chem. Commun.* **1994**, 1509. (d) Gómez-Romero, P.; Lira-Cantu, M. *Adv. Mater.* **1997**, *9*, 144. (e) Otero, T. F.; Cheng, S. A.; Huerta, C. F. *J. Phys. Chem. B* **2000**, *104*, 10522. (f) Otero, T. F.; Cheng, S. A.; Alonso, D.; Huerta, F. *J. Phys. Chem. B* **2000**, *104*, 10528. (g) Cheng, S. A.; Otero, T. F.; Coronado, E.; Gomez-Garcia, C. J.; Martinez-Ferrero, E.; Gimenez-Saiz, C. *J. Phys. Chem. B* **2002**, *106*, 7585.
(15) Liu, S.; Kurth, D. G.; Bredenkotter, B.; Volkmer, D. *J. Am. Chem. Soc.* **2002**, *124*, 12279.
(16) (a) Judeinstein, P. *Chem. Mater.* **1992**, *4*, 4. (b) Mayer, C. R.; Cabuil, V.; Lalot, T.; Thouvenot, R. *Angew. Chem., Int. Ed. Engl.* **1999**, *38*, 3672. (c) Mayer, C. R.; Thouvenot, R.; Lalot, T. *Chem. Mater.* **2000**, *12*, 257. (d) Schroden, R. C.; Blanford, C. F.; Melde, B. J.; Johnson, B. J. S.; Stein, A. *Chem. Mater.* **2001**, *13*, 1074. (e) Johnson, B. J. S.; Stein, A. *Inorg. Chem.* **2001**, *40*, 801. (f) Moore, A. R.; Kwen, H.; Beatty, A. B.; Maatta, E. A. *Chem. Commun.* **2000**, 1793. (g) Schubert, U. *Chem. Mater.* **2001**, *13*, 3487.
(17) Bunz, U. H. F. *Chem. Rev.* **2000**, *100*, 1605.

Scheme 1. Two Synthetic Routes to Conjugated Polymer Hybrids

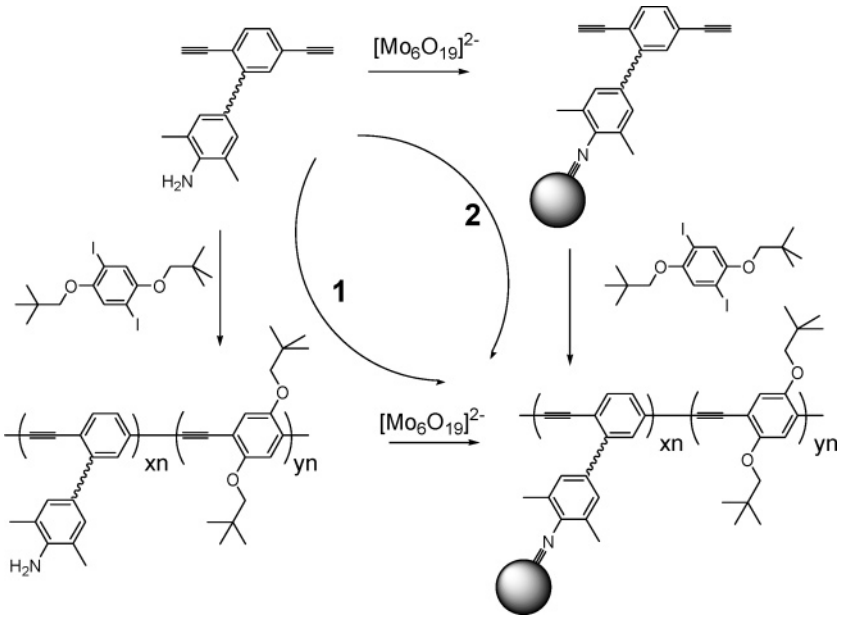

Scheme 2. Synthesis of Hybrid Monomer 6

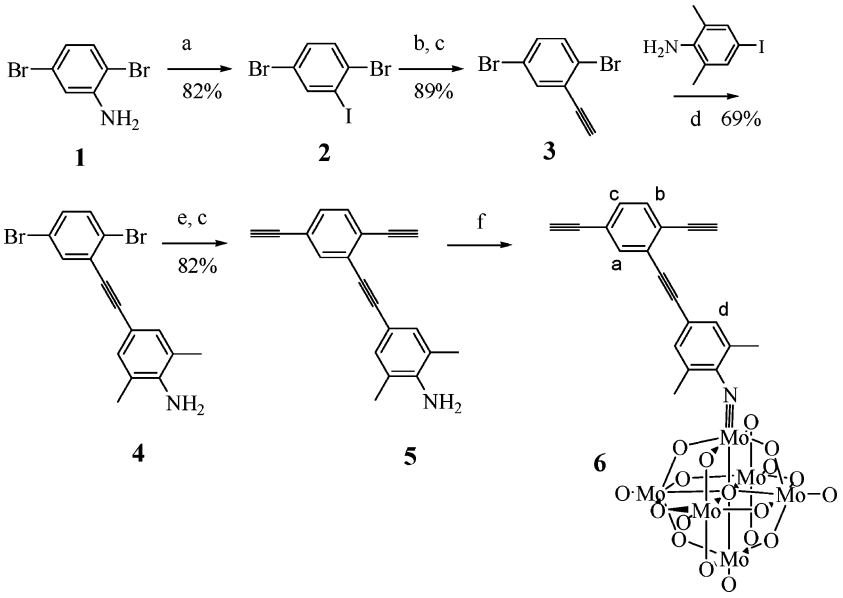

4-iodo-2,6-dimethylaniline to give compound **4** in 69% yield. Both steps were carried out at room temperature.[19] Another Sonogashira coupling reaction, at an elevated temperature this time, converts the two bromo groups in **4** to two ethynyl groups (**5**). The hybrid monomer was finally prepared by the reaction of the arylamine with the hexamolybdate cluster under conditions previously reported.[20]

Monomer **6** was characterized by ^{1}H NMR and X-ray single-crystal diffraction. In its ^{1}H NMR spectrum, the two alkynyl protons give two singlets at 3.85 and 3.56 ppm. In the aromatic region, two singlets at 7.60 and 7.26 ppm and two doublets at 7.53 and 7.45 ppm are observed, which can be assigned to protons a, d, b, and c, respectively (see Scheme 2 for hydrogen labeling). Protons in the tetrabutylammonium counterion appear at chemical shifts of 0.96, 1.37, 1.57, and 3.09 ppm.

Figure 2 shows the X-ray crystal structure of the anion in **6**. Compound **6** crystallizes in the orthorhombic space group $P2_12_12_1$. The imido linkage between the organic segment and the cluster shows features common to all imido derivatives of hexamolybdates, such as a linear Mo−N−C bond angle and a shorter O^c to imido bearing Mo bond length than to its para Mo atom, etc.[21] The two phenyl rings are significantly twisted away from the planar configuration as a large dihedral angle of 46.5° is observed.

(18) (a) Golt, A.; Ziener, U. *J. Org. Chem.* **1997**, *62*, 6137. (b) Huang, S.; Tour, J. M. *Tetrahedron Lett.* **1999**, *40*, 3347.
(19) Sonogashira, K.; Tohda, Y.; Hagihara, N. *Tetrahedron Lett.* **1975**, 4467.
(20) Wei, Y.; Xu, B.; Barnes, C. L.; Peng, Z. *J. Am. Chem. Soc.* **2001**, *123*, 4083.
(21) (a) Gouzerh, P.; Proust, A. *Chem. Rev.* **1998**, *98*, 77. (b) Strong, J. B.; Yap, G. P. A.; Ostrander, R.; Liable-Sands, L. M.; Rheingold, A. L.; Thouvenot, R.; Gouzerh, P.; Maatta, E. A. *J. Am. Chem. Soc.* **2000**, *122*, 639. (c) Stark, J. L.; Young, V. G., Jr.; Maatta, E. A. *Angew. Chem., Int. Ed. Engl.* **1995**, *34*, 2547.

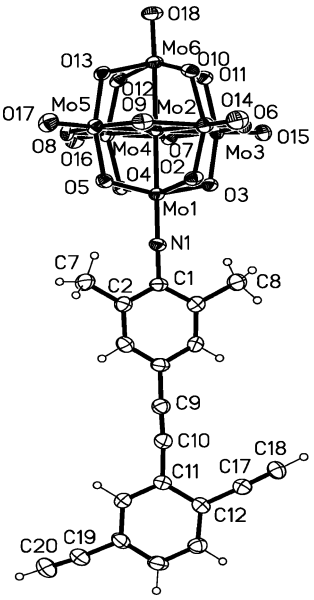

Figure 2. Anion structure of **6**. The displacement ellipsoids were drawn at the 50% probability level. Selected bond lengths (Å) and bond angles (deg): Mo1−N1 1.738(3), Mo1−O1 2.207(3), Mo2−O14 1.692(3), Mo2−O1 2.341(3), Mo3−O15 1.698(3), Mo3−O1 2.343(3), Mo4−O16 1.700-(3), Mo4−O1 2.345(3), Mo5−O17 1.685(3), Mo5−O1 2.325(3), Mo6−O18 1.687(3), Mo6−O1 2.349(3), N1−C1 1.380(5), and Mo1−N1−C1 178.7(3).

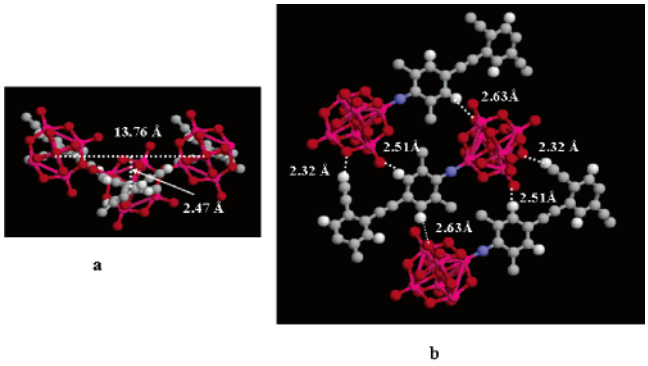

Figure 3. Trimer structure assembled through multiple hydrogen bonds (most of the hydrogen atoms are omitted for clarity), viewed along the direction of the molecular axis (a) or perpendicular to the molecular axis (b).

Within the lattice of **6**, the hybrid anions are grouped into trimers. As shown in Figure 3, each trimer contains two molecular rods aligning parallel to each other with a separation distance of 13.76 Å, while the third parallel rod with head and tail reversed is located right between, but off the center orthogonally by 2.47 Å (see Figure 3a, viewing the trimer along the molecular axis). The three anions are held together by multiple nonconventional C−H···O hydrogen bonds (Figure 3b),[22] among which the strongest is between the μ_2-O of the cluster and the alkylnyl hydrogen whose separation distance is only 2.32 Å. Other hydrogen bonds include those between an Ar−H and a terminal oxygen of the cluster (2.51 Å) and an Ar−H and a μ_2-O of the cluster (2.63 Å). Similar weak hydrogen bonds have been observed in the crystal structures of a few other imido derivatives of hexamolybdates.[23]

To prepare hybrid polymers with POM clusters linked through a flexible linkage, monomer **13** was designed, and its synthetic approach is shown in Scheme 3. Starting from 4-methoxyphenol, compound **7** was prepared in 95% yield. The Sonogashira coupling of **7** with **8**, which was synthesized by protecting the arylamine group of 4-iodo-2,6-dimethylaniline with phthalimide, gave compound **9** in 90% yield. Catalytic hydrogenation of the triple bond in **9** with Pd/C produced compound **10** in excellent yields. Subsequent iodination on **10** occurred selectively on the phenyl ring with dialkoxy substituents, giving **11** in 84% yield. Compound **12** was then prepared by reacting **11** with hydrazine to regenerate the arylamine group. The imido formation reaction of **12** with hexamolybdate occurred smoothly in refluxing acetonitrile in the presence of DCC. Unfortunately, it was found to be rather difficult to obtain a significant amount of monomer **13** in high purity (see Supporting Information for the ^{1}H NMR spectrum of **13**). There are residual parent hexamolybdate clusters that could not be eliminated completely due to the poor crystallization tendency of compound **13**. The existence of impurity in **13** complicates the stoichiometric calculation and thus limits the degree of polymerization. In view of the perspective that free hexamolybdate clusters may be easily separated from the final targeted polymers, an alternative synthetic approach combining the hybridization and the subsequent polymerization in one pot was thus explored.

As shown in Scheme 4, the one-pot synthesis started with compound **12** (or **5**). Stoichiometric calculation for polymerization was therefore based on compounds **12** (or **5**), **14**, and **15**. Thus, compound **12** (or **5**) was first allowed to react with excess hexamolybdate in acetonitrile to ensure complete functionalization of all arylamine groups. After the reaction, the solvent (acetonitrile) was stripped off under vacuum. A mixed solvent of THF and DMF, together with compounds **14**, **15**, and the catalyst system, was then added to promote polymerization. After polymerization, the reaction mixture was filtered to remove excess hexamolybdates, and the filtrate was poured into acetonitrile. Polymer precipitated while free hexamolybdate clusters remained in solution. To be consistent, both sets of polymers (**Ia**, **Ib**, **IIa**, and **IIb**) were synthesized by the previous approach. For comparison, a PPE polymer that does not contain POM pendants (polymer **III**) was also synthesized by the coupling reaction of **14** with **15**.

Structural Characterizations. All polymers are soluble in acetone, DMSO, chloroform, and dichloromethane but insoluble in acetonitrile, methanol, and THF. The ^{1}H NMR spectra of compounds **5**, **6**, and polymer **Ia** are shown in Figure 4.

Compound **5** in acetone-d_6 shows singlets at 3.82, 4.07, and 4.70 ppm. The first two signals can be assigned to the two ethynyl protons, while the third singlet is attributed to the arylamine group. After hybridization and subsequent

(22) Desiraju, G. R.; Steiner, T. *The Weak Hydrogen Bond In Structural Chemistry and Biology* (International Union of Crystallography, Monographs on Crystallography, No. 9); Oxford University Press: Oxford, 2001.

(23) (a) Stark, J. L.; Young, V. G., Jr.; Maatta, E. A. *Angew. Chem., Int. Ed. Engl.* **1995**, *34*, 2547. (b) Xu, L.; Lu, M.; Xu, B.; Wei, Y.; Peng, Z.; Powell, D. R. *Angew. Chem., Int. Ed.* **2002**, *41*, 4129.

Scheme 3. Synthesis of Monomer 13

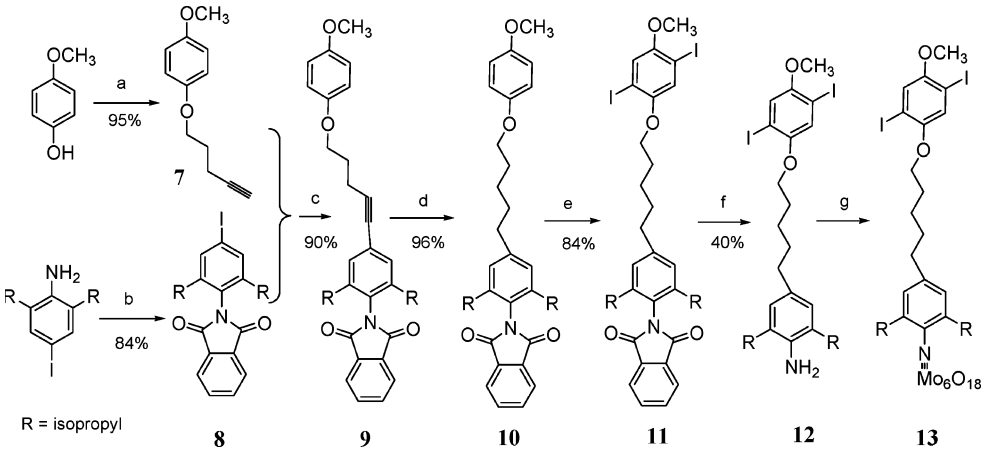

Scheme 4. Synthesis of Hybrid Conjugated Polymers

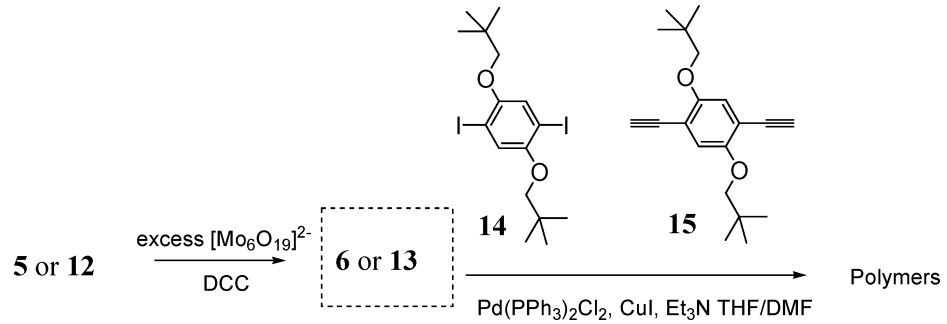

polymerization, the arylamine signal disappeared completely, and new peaks corresponding to the tetrabutylammonium counterions appeared at 3.40, 1.78, 1.44, and 0.95 ppm, indicating rather complete N−Mo imido bond formation

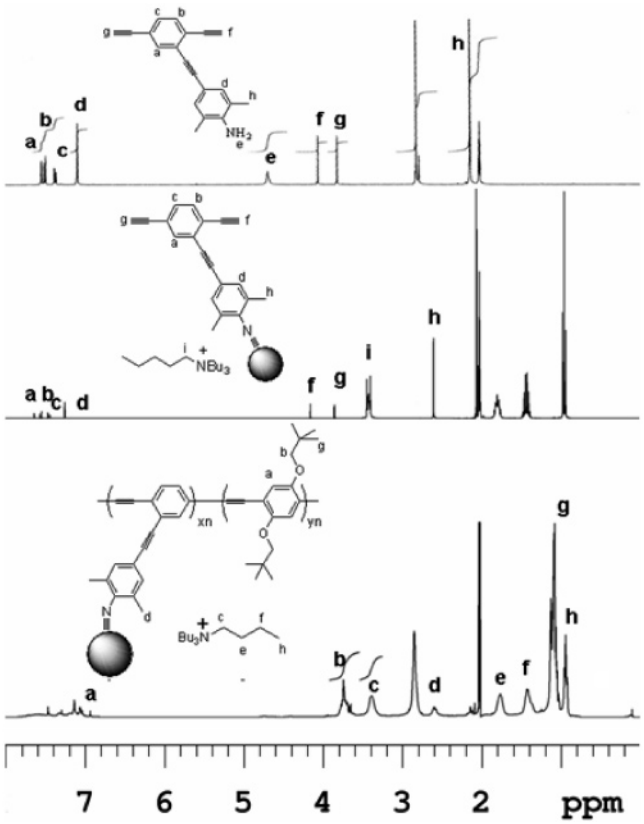

Figure 4. ^{1}H NMR spectra of **5**, **6**, and polymer **Ia** in acetone-d_6.

Table 1. Theoretical and experimental Mo content of the four hybrid polymers

	IIa	IIb	Ia	Ib
Mo% (theoretical)	18.57	13.74	19.14	14.05
Mo% (experimental)	15.09	10.40	16.07	10.30

during the hybridization process. The ^{1}H NMR spectra of **Ia** and **Ib** show no ethynyl proton signals, while new peaks corresponding to the alkoxy side chains appeared at 3.78 and 1.22 ppm. The lack of an alkynyl proton signal indicates either high degrees of polymerization for polymers **Ia** and **Ib** or dominant iodo end groups in these polymers. The methylene protons in the neopentoxy substituents appeared at 3.78 ppm. The integration ratio of the signals at 3.78 ppm (-OCH_2-) versus the one at 3.40 ppm (-NCH_2-) for polymer **Ia** is 1.2, consistent with the theoretical value of 1.25. The ^{1}H NMR spectrum of monomer **12** shows two singlets in the aromatic range at 6.84 and 7.17 ppm (see Supporting Information). The amine protons give a singlet at 3.60 ppm. After one pot hybridization/polymerization, the amine signal again completely disappeared. New signals corresponding to the counterion protons again appeared.

Elemental analysis of polymers confirms the existence of clusters. As shown in Table 1, while the analyzed Mo contents are consistently lower than the theoretical values by about 3−4%, which may be due to the lower reactivity of monomers **6** and **13** than those of **15** and **14**, respectively, the Mo contents do follow the trend of loading ratios (e.g., polymers **Ia** and **IIa** have higher Mo contents than **Ib** and **IIb**).

The attachment of clusters to the polymer backbone is also confirmed by IR measurements. As shown in Figure 5, the

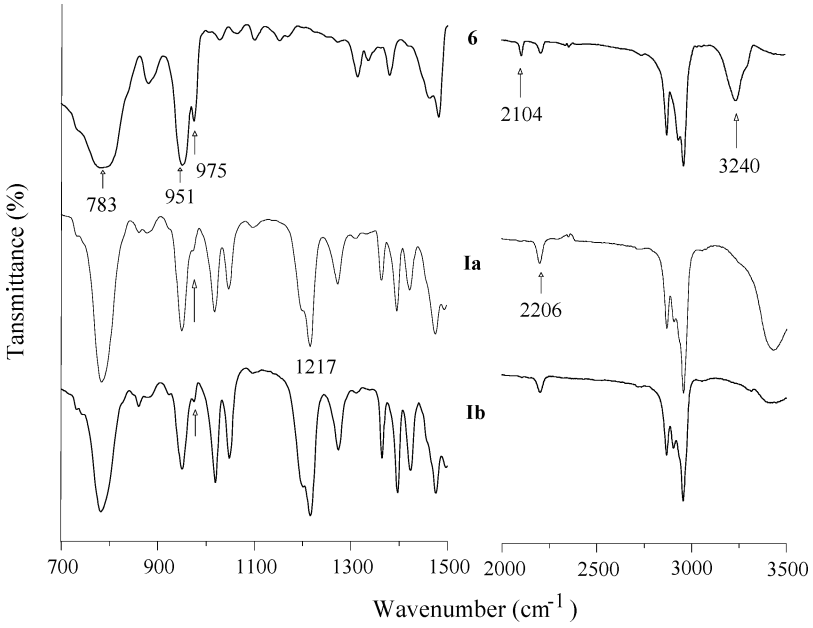

Figure 5. IR spectra of compound **6** and polymers **Ia** and **Ib**.

IR spectrum of monomer **6** shows absorption bands at 783, 951, and 975 cm^{-1}, which are typical absorptions of imido derivatives of hexamolybdates.[24] Two characteristic stretching bands for the C≡C triple bonds appear at 2104 and 2206 cm^{-1}, attributable to the terminal and internal alkyne bonds, respectively. The absorption centered at 3240 cm^{-1} corresponds to the stretching vibration of the alkynyl hydrogen. For polymers **Ia** and **Ib**, however, the bands at 2104 and 3240 cm^{-1} have disappeared, indicating complete incorporation of monomer **6** into the polymer backbone. The three bands at 783, 951, and 975 cm^{-1} are clearly shown in the IR spectra of polymers **Ia** and **Ib**, signaling the existence of imido-functionalized hexamolybdates in the polymers. As compared to **6**, the IR spectra of polymers **Ia** and **Ib** show new bands, such as the one at 1217 cm^{-1}, which can be assigned to the stretching mode of C−O bonds. The relative intensity of the band at 951 cm^{-1} versus the one at 1217 cm^{-1} for **Ia** is higher than that of **Ib**, indicating that the percentage amount of functionalized clusters in polymer **Ia** is higher than that of **Ib**, consistent with experimental loading ratios. The IR spectra of polymers **IIa** and **IIb** are very similar to those of **Ia** and **Ib**. A clear, well-resolved peak at 975 cm^{-1} is observed for both **IIa** and **IIb**, indicating the existence of Mo−N imine bonds.

Molecular Weights. The molecular weights of these hybrid polymers were evaluated by viscometry, gel-permeation chromatography (GPC), and light-scattering measurements. The GPC measurements, which were carried out at 30 °C using a Styrogel 4E column with DMF as the eluent and polystyrene as the standards, give average molecular weights of 169 and 176 kDa for **Ia** and **IIa**, respectively. It is noted that the separation of such hybrid polymers in GPC columns is very poor as exceedingly narrow molecular weight distributions (<1.01) for both **Ia** and **IIa** were obtained (see Supporting Information). While the molecular weights based on GPC (relative to polystyrene standards, which are clearly not good standards for the rigid polymers) may be questionable, light-scattering analysis, performed on a DAWN EOS system from Wyatt Technologies with an Optilab rEX DRI detector, gives an average molecular weight of 15.7 kg/mol for **Ia**, indicating that polymers are indeed obtained. Realizing that the poor GPC separation of hybrid polymers may be due to the existence of ionic clusters, we have attempted to break the Mo−N bonds and then subject the resulting cluster-stripped polymers for GPC analysis. Thus, 0.5 mL of CF_3COOH was added to a 5% DMF solution of a hybrid polymer (3 mL, wt %). Dark red precipitates were formed in 10 min and the color of the solution changed from red to yellow. The resulting polymer precipitates, unfortunately, are not soluble in any organic solvents and thus could not be subjected to GPC analysis. The intrinsic viscosity for polymer **Ia**, measured using an Ubbelohde capillary viscometer at 30 °C, is 39 cm^3/g.

Thermal Properties. Thermal properties of **6** and the hybrid polymers were studied by thermogravimetric analysis (TGA), and the results are listed in Table 2. All four hybrid polymers are thermally stable up to 220 °C under nitrogen, as is monomer **6**. The decomposition of the four hybrid polymers appears to occur in two stages with the first weight loss of about 25% occurring rapidly within a 10 degree range, followed by a slower but significantly larger weight loss of about 50%. Beyond 450 °C, no further weight loss is observed for all four polymers up to 600 °C. By comparing the TGA thermograms of polymers **Ia** and **Ib** with that of monomer **6**, as shown in Figure 6, one may conclude, with reasonable confidence, that the initial decomposition is associated with the attached hybrid cluster while the second decomposition process is attributed to the breakdown of the polymer backbone. The residual amounts for polymers **Ia** and **Ib** are 26 and 22%, respectively, which correspond well to their respective cluster anion contents of 29 and 21% (assuming the thermally decomposed residue is MoO_3). It

(24) Li, Y.; Hao, N.; Wang, E.; Yuan, M.; Hu, C.; Hu, N.; Jia, H. *Inorg. Chem.* **2003**, *42*, 2729.

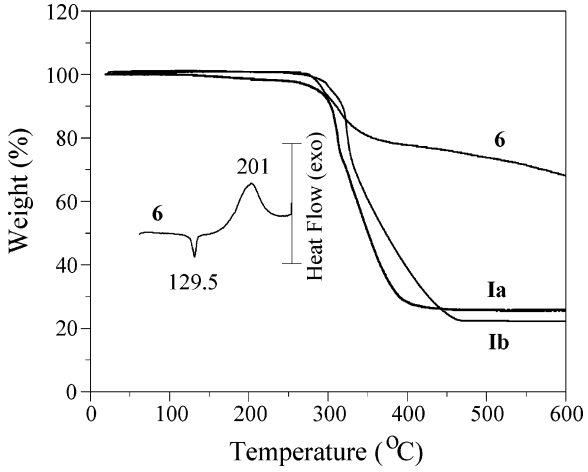

Figure 6. TGA thermograms of **6**, **Ia**, and **Ib**. The inset is the DSC thermogram of **6**.

should be pointed out that monomer **6** shows clearly different decomposition behavior. After the initial 20% weight loss, the second stage weight loss for **6**, as compared to those of hybrid polymers, is much shallower and continues up to 600 °C. No leveling-off is observed. The residual amount for monomer **6** at 600 °C is 68%, much higher than its cluster anion content of 53.5%. Clearly, a certain amount of organic components survived at such a high temperatures. Examining its DSC thermogram (shown in Figure 6 as an inset), one notices a relatively sharp melting transition at 129.5 °C (peak temperature) and an exothermal transition peaking around 201 °C. Considering the fact that no weight loss occurred during these transitions, the exothermal process is likely due to chemical reactions associated with the terminal alkynes. Similar exothermal transitions have been observed for other terminal alkyne-containing hybrids such as 4-ethynyl-2,6-dimethylimidohexamolybdate. It is possible that the thermal cross-linking of terminal alkynes results in an organic π-carbon network that is more thermally stable. The percentage amount including the cluster anion portion and the π-carbon portion (excluding the counterions and the alkyl groups) in **6** is indeed 68%. The decomposition of polymers **IIa** and **IIb** shows similar features to that of **Ia** and **Ib**.

Electrochemistry. The electrochemistry of the hybrid polymers was studied by cyclic voltammetry. The experiments were carried out in acetonitrile at room temperature under the protection of Argon using a BAS Epsilon EC electrochemical station employing a 1 mm^2 Pt disk as the working electrode, Ag/Ag$^+$ electrode (0.01 M $AgNO_3$) as the reference electrode, and a Pt wire as the counter electrode. $[Bu_4N]PF_6$ was the supporting electrolyte, and the scan rate was 30 mV s^{-1}. For polymer samples, thin films were cast on the platinum disk working electrode. For other samples, acetonitrile solutions were used. The results are listed in Table 2. Figure 7 shows the cyclic voltammograms of monomer **6** and polymers **Ib** and **IIa**. Monomer **6** shows one reversible one-electron reduction wave at -0.905 V ($\Delta E_p = 0.13$ V). Under the same conditions, the free hexamolybdate cluster, $[Mo_6O_{19}][Bu_4N]_2$, shows one reversible one-electron reduction wave at -0.692 V ($\Delta E_p = 0.09$ V). Scanning in the range of 0 to -2.5 V, all four hybrid polymers reveal one quasi-reversible reduction wave at -2.10 V ($E_{onset} = -1.83$ V), which can be attributed to the reduction of the conjugated polymer backbone since a similar reduction wave is observed for polymer **III** (Table 2). There is also a very small and yet clear reduction wave at $E_{pc} = -1.03$ V, as shown in the expanded view of the CV curve of **IIa** in Figure 7. This process is assigned to the reduction of the pendant clusters, and the irreversibility is consistent with other imido derivatives of hexamolybdates that are known to undergo an irreversible reduction process in the range of -2.0 to -2.5 V.[21c] The irreversible reduction process becomes reversible when the scanning range is shorted to 0 to approximately -1.5 V, which is shown clearly in Figure 7 for both **Ib** and **IIa**. No reduction wave corresponding to free hexamolybdate clusters can be identified, indicating that all clusters are attached to the polymer backbone as pendants and that free hexamolybdate clusters are negligible. All four hybrid polymers exhibit such a reversible reduction wave in the range of -0.93 to -0.95 V (see Table 2), while polymer **III** shows no electrochemical process from 0 to -1.2 V. During the anodic scan, all

Table 2. Thermal, Electrochemical, and Optical Properties of Hybrid Conjugated Polymers

	T_d[a] (°C)	CV (V vs Ag/Ag$^+$) E_{red}	CV (V vs Ag/Ag$^+$) E_{ox}[b]	λ_{max}^{abs} (nm)	λ_{max}^{em} (nm)	η (%)[c]
Ia	242	−0.93, −2.06	0.58	406	466	0.04
Ib	250	−0.94, −2.04	0.60	410	468	0.09
IIa	220	−0.97, −1.83	0.57	444	473	0.16
IIb	253	−0.96, −1.98	0.56	442	474	0.23
III	260	−2.04	0.55	425	472	0.29

[a] Onset decomposition temperature. [b] Onset voltage (irreversible oxidation). [c] Fluorescence quantum efficiencies measured in dilute methylene chloride solutions.

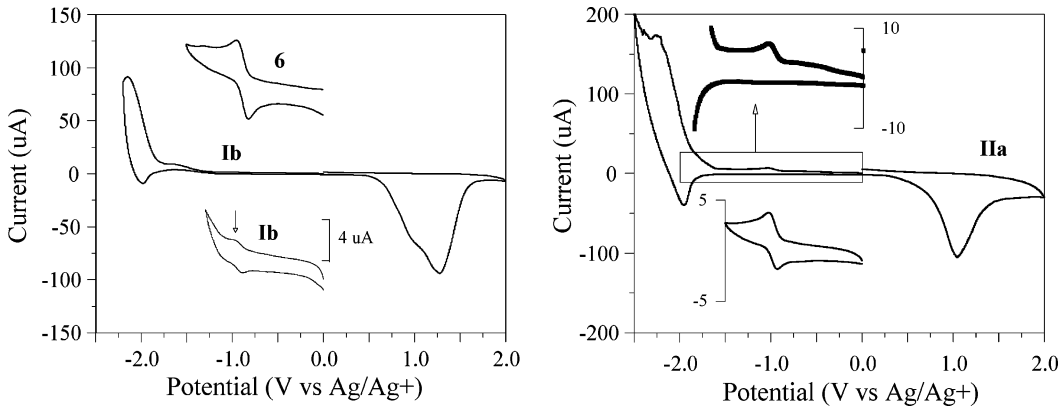

Figure 7. Cyclic voltammograms of monomer **6** and polymers **Ib** and **IIa**. UV/vis absorption spectra of **6** and the hybrid polymers.

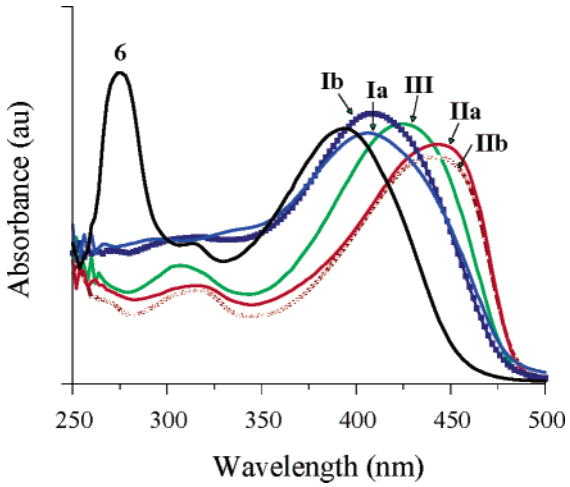

Figure 8. UV/Vis absorption spectra of **6** and the hybrid polymers.

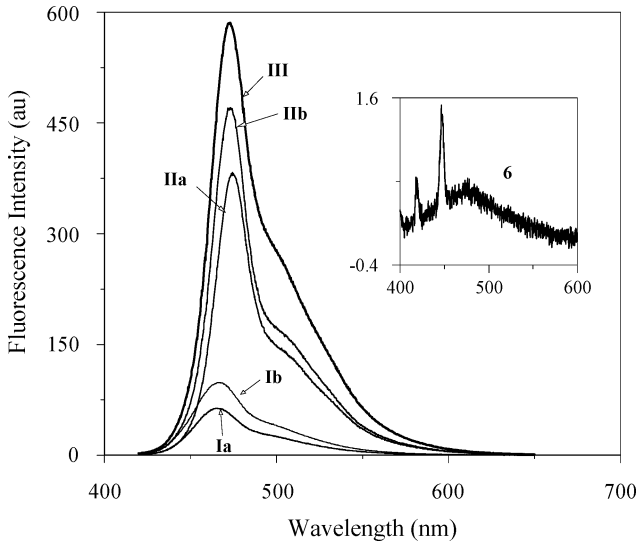

Figure 9. Fluorescence emission spectra of polymer **III** and the four hybrid polymers. The inset is the FL spectrum of monomer **6**.

polymers exhibit broad irreversible oxidation waves centered around 1.2 V, which are attributed to the oxidation of the conjugated polymer backbones.

Electronic Properties. Figure 8 shows the UV/vis absorption spectra of monomer **6** and the five polymers. Compound **6** shows a broad absorption band in the visible range with a λ_{max} of 394 nm, which is assigned to the ligand-to-metal charge-transfer transition associated with the Mo−N π-bonding and the $\pi\angle\pi^*$ transition of the organic π-extended segment. There is also an intense and relatively sharp absorption centered at 276 nm, which is also found in the absorption spectrum of compound **5** but not **4**. This absorption is thus attributed to the $\pi\angle\pi^*$ transition associated with the *p*-diethynylphenyl segment. After polymerization, this absorption peak has disappeared, while the λ_{max} values of the polymers red-shifted. The λ_{max} values of polymers **Ia**, **Ib**, **IIa**, and **IIb** are 406, 410, 444, and 442, respectively. Polymer **III**, without POM pendants, has a λ_{max} of 425 nm. The slightly lower maximum absorption wavelengths for set **I** polymers than that of **III** is likely due to the rigid and bulk substituents that distort chain conjugation. The lack of alkoxy substitution on the chain-participating phenyl ring in **6** may also result in a blue-shifted $\pi\angle\pi^*$ transition. Set **II** polymers, on the other hand, have red-shifted $\pi\angle\pi^*$ transitions. In set **II** polymers, POM clusters hang flexibly and away from the backbone. In addition, the chain-participating phenyl ring in **12** or **13** has a methoxy substituent that is much less sterically demanding than the neopentoxy groups in polymer **III**. The PPE backbone in set **II** polymers is thus less distorted, leading to lower band gaps.

Unlike previously reported main-chain POM-containing polymers that exhibit no fluorescence,[12] conjugated polymers with POM pendants do show fluorescence from the polymer backbone. As shown in Figure 9, all four hybrid polymers show very similar fluorescence emission spectra to that of polymer **III**, except for a slight blue shift for set **I** polymers. Monomer **6**, however, exhibits negligible fluorescence (Figure 9, inset). While all hybrid polymers are fluorescent, the fluorescence intensities and quantum yields of polymers **Ia** and **Ib** are significantly lower than that of polymer **III**. Polymers **IIa** and **IIb**, on the other hand, are still highly fluorescent, although their fluorescence quantum yields are also lower than that of polymer **III**. As listed in Table 2, the fluorescence quantum yield of polymer **III** in dilute methylene chloride solution is 0.29, while the fluorescence quantum yields of polymers **Ia**, **Ib**, **IIa**, and **IIb** are 0.04, 0.09, 0.16, and 0.23, respectively. Adding hexamolybdate clusters to the solution of polymer **III**, even up to 1 equiv of the repeating unit, exhibits little quenching effect on the polymer fluorescence, indicating that the fluorescence quenching is indeed promoted by covalent binding of the clusters to the polymer backbone. Within each set, the higher the cluster loading ratio in the polymer, the lower the fluorescence quantum yield. Clearly, the covalently linked POM clusters, particularly those with conjugated linkages, exhibit significant fluorescence quenching. It is believed that the photoinduced electron transfer from the PPE backbone to the POM clusters accounts for the fluorescence quenching. It is likely that the through-bond electron-transfer mechanism dominates for set **I** polymers, while for set **II** polymers, only the through-space mechanism is possible, which may not be as efficient.

Conclusions

Hexamolybdate clusters have been covalently attached, for the first time, to the side chains of conjugated polymers. Two sets of such hybrid conjugated polymers have been prepared, one (**Ia** and **Ib**) with the clusters linked to the conjugated backbone through a rigid conjugated bridge, the other (**IIa** and **IIb**) through flexible alkyl chains. Within each set, polymers with different cluster loading ratios have been prepared. While pure monomer **6**, which has remote bifunctionality, has been successfully prepared, a convenient one-pot synthesis has been utilized to prepare all hybrid polymers. The covalent attachment of POM clusters has been confirmed by ^{1}H NMR, FTIR, and cyclic voltammetry measurements. These hybrid polymers are thermally stable up to 220 °C. Set **I** polymers (**Ia** and **Ib**) exhibit maximum absorption wavelengths (λ_{max}) around 410 nm, while set **II** polymers (**IIa** and **IIb**) show higher λ_{max} values, around 440 nm. Fluorescence studies show that side-chain POM pendants

linked through conjugated bridges exhibit a much higher fluorescence quenching effect than those with flexible alkyl bridges, indicating that the through-bond photoinduced electron transfer may be the dominant mechanism for fluorescence quenching. With efficient fluorescence quenching that results in free charge carriers residing in different structural units (positively charged holes in the PPE backbone and negatively charged electrons in the POM clusters), these hybrid polymers may have potential for applications in photovoltaic (PV) cells.

Experimental Procedures

Compounds 14 and **15** were prepared according to literature procedures.[25] THF was purified by distillation over sodium chips and benzophenone. Triethylamine was distilled over CaH_2. All of the other chemicals were purchased either from ACROS or Aldrich and were used as received unless otherwise stated. The ^{1}H NMR spectra were collected on a Varian 400 MHz FT NMR spectrometer. Thermal analyses were performed on Shimadzu DSC-50 and TGA-60. GPC measurements were performed at 30 °C on a Waters setup (a Waters 210 pump, a Waters R401 differential refractometer, and a styragel 4E column) with DMF as the eluent. The calibration curve was determined by use of five polystyrene standards from 800 to 90 000. Light-scattering analysis was carried out on a DAWN EOS system with an Optilab rEX DRI detector from Wyatt Technologies. FT-IR spectra were obtained from samples dispersed in KBr pellets and recorded on an IR100 FT-IR spectrometer (Thermo-Nicolet Co.). A Hewlett-Packard 8452A diode array spectrophotometer was used to record the UV/vis absorption spectra. Photoluminescence properties were measured using a Shimadzu RF-5301PC spectrofluorophotometer. Cyclic voltammetry (CV) studies were carried out in acetonitrile at room temperature under the protection of nitrogen using a BAS Epsilon EC electrochemical station employing a 1 mm^2 Pt disk as the working electrode, Ag/Ag^+ electrode (0.01 M $AgNO_3$) as the reference electrode, and a Pt wire as the counter electrode. $[Bu_4N]PF_6$ was the supporting electrolyte, and the scan rate was 30 mV s^{-1}. For monomer **6**, the measurements were done using its acetonitrile solutions. For polymers, a thin polymer film was first cast onto the Pt disk working electrode, and the voltammograms were recorded in acetonitrile.

Compound 2. 2,5-Dibromoaniline (9.0 g, 35.9 mmol) and hydrochloric acid (15 mL, 37%) were dissolved in 38 mL of acetonitrile (38 mL). The solution was cooled to 5−10 °C. To this solution was added dropwise an aqueous solution of sodium nitrite (3.2 g, 46.4 mmol in 15 mL of water). The resulting mixture was stirred at 5−10 °C for 20 min and then poured into a solution of potassium iodide (60 g, 0.36 mol) in water (75 mL). The mixture was set undisturbed for 20 min and was then extracted with methylene chloride (3 × 300 mL). The organic layer was collected, washed with water (3 × 400 mL), and dried over magnesium sulfate. The solvent was evaporated to yield crude product, which was purified by column chromatography (Al_2O_3, neutral, hexane as the eluent) to afford compound **2** (10.6 g, 82%) as a colorless liquid, which solidified after 24 h. Mp 37−38.5 °C. ^{1}H NMR (400 MHz, $CDCl_3$, 25 °C): δ 7.28−7.35 (m, 1 H, Ar−H), 7.45 (d, J = 8.5 Hz, 1 H, Ar−H), 7.97 (d, J = 2.5 Hz, 1 H, Ar−H). ^{13}C NMR ($CDCl_3$, 62.5 MHz) δ 102.3, 121.4, 124.3, 128.8, 132.7, 133.7.

Compound 3. A mixture containing compound **2** (5.0 g, 13.8 mmol), trimethylsilylacetylene (1.63 g, 16.6 mmol), bis(triphenylphosphine)palladium (II) chloride (0.3 g, 0.43 mmol), copper (I) iodide (0.18 g, 0.95 mmol), triethylamine (4 mL), and THF (40 mL) was stirred at room temperature overnight and was then poured into hexanes (300 mL). The resulting mixture was washed with water (3 × 300 mL). The organic layer was collected and filtered through Celite 545 (Fisher Co.). The filtrate was stripped of solvent to give 4.16 g of the trimethylsilyl-protected precursor, which was then desilylated by the following procedure: tetrabutylammonium fluoride (1 M solution in THF, 20 mL, 20 mmol) was added to a solution of 2,5-dibromotrimethylsilylethynylbenzene (4.16 g) in methylene chloride (50 mL). The resulting mixture was stirred at room temperature for 15 min and was then poured into hexane (300 mL). The resulting solution was washed with water (3 × 300 mL), and the organic layer was collected, dried over magnesium sulfate, and then stripped of solvent to afford crude product. The crude product was purified by flash chromatography (Al_2O_3, neutral, hexane as the eluent) to yield compound **3** (reddish solid, 3.2 g, 89%). Mp 43−44 °C. ^{1}H NMR (400 MHz, $CDCl_3$, 25 °C): δ 3.42 (s, 1 H, −CCH), 7.33 (dd, J = 8.4 Hz, 2.4 Hz, 1 H, Ar−H), 7.44 (d, J = 8.8 Hz, 1 H, Ar−H), 7.65 (d, J = 2.4 Hz, 1 H, Ar−H). ^{13}C NMR ($CDCl_3$, 100 MHz) δ 80.8, 83.3, 120.8, 124.5, 126.4, 133.3, 133.9, 136.7.

Compound 4. Compound **3** (4.6 g, 17.7 mmol), 2,6-dimethyl-4-iodo-aniline (4.0 g, 16.2 mmol), bis(triphenylphosphine)palladium (II) chloride (0.34 g, 0.48 mmol), and copper(I) iodide (0.17 g, 0.9 mmol) were added to a 100 mL two-neck flask. The flask was evacuated and backfilled with nitrogen three times. THF (30 mL) and triethylamine (3 mL) were then added to the flask with a syringe. After being stirred at room temperature for 10 h, the reaction mixture was poured into water (400 mL) and extracted with methylene chloride (3 × 200 mL). The organic layer was collected, dried over Na_2SO_4, and stripped of solvent to give the crude product, which was further purified by chromatography (silica gel, eluent?) to yield 4.24 g of compound **4** (gray solid, 69%, mp 120−122 °C). ^{1}H NMR (400 MHz, $CDCl_3$, 25 °C): δ 2.18 (s, 6 H, Ar−CH_3), 3.82 (s, 2 H, Ar−NH_2), 7.19 (s, 2 H, Ar−H), 7.23 (dd, J = 8.4, 2.4 Hz, 1 H, Ar−H), 7.43 (d, J = 8.8 Hz, 1 H, Ar−H), 7.63 (d, J = 2.4 Hz, 1 H, Ar−H). ^{13}C NMR ($CDCl_3$, 62.5 MHz) δ 17.4, 84.9, 97.2, 110.7, 120.6, 121.4, 123.9, 128.1, 131.5,133.5, 135.1, 136.4, 144.2.

Compound 5. A mixture containing compound **4** (1.6 g, 4.2 mmol), triisopropylsilylacetylene (1.84 g, 10.1 mmol), bis(triphenylphosphine)palladium (II) chloride (0.12 g, 0.17 mmol), copper (I) iodide (60 mg, 0.32 mmol), triethylamine (30 mL), and THF (10 mL) was stirred at 80 °C under nitrogen for 48 h. After being cooled to room temperature, the mixture was poured into hexane (300 mL) and was then washed with water (3 × 300 mL). The organic layer was collected and filtered through Celite 545 (Fisher Co.). The filtrate was stripped of solvent. The resulting solids were purified by chromatography (Al_2O_3, neutral, hexanes/ethyl acetate = 5:1 as the eluent) to give the triisopropylsilyl protected coupling product (pale solid, 1.8 g), which was then desilylated using a procedure similar to the one described in the synthesis of compound **3** to yield compound **5** in 82% overall yield (brown solid, 0.93 g, mp 143−145 °C). ^{1}H NMR (CD_3COCD_3, 400 MHz, 25 °C): δ 2.14 (s, 6 H, Ar−CH_3), 3.82 (s, 1 H, -CCH), 4.07 (s, 1 H, -CCH), 4.70 (s, 2 H, Ar−NH_2), 7.10 (s, 2 H, Ar−H), 7.38 (dd, J = 6.4 and 1.6 Hz, 1 H, Ar−H), 7.51 (d, J = 8.0 Hz, 1 H, Ar−H), 7.55 (s, 1 H, Ar−H). ^{13}C NMR ($CDCl_3$, 100 MHz) δ 17.6, 79.4, 82.2, 82.7, 82.8, 85.0, 96.1, 111.5, 121.6, 122.6, 124.5, 127.7, 130.6, 132.1, 132.6, 135.1, 144.0. Anal. Calcd for $C_{20}H_{15}N$: C, 89.18; H, 5.61. Found: C, 88.87; H, 5.46.

Compound 6. A mixture containing compound **5** (0.1000 g, 0.3715 mmol), DCC (0.0919 g, 0.446 mmol), $[Mo_6O_{19}]$ $[N(C_4H_9)_4]_2$ (0.608 g, 0.446 mmol), and CH_3CN (5 mL) was refluxed for 12 h. After being cooled to room temperature, the reaction mixture was

(25) Bao, Z.; Chen, Y.; Cai, R.; Yu, L. *Macromolecules* **1993**, *26*, 5281.

filtered to remove the white precipitates (side product urea). The filtrate was stripped of solvent. Acetone (5−7 mL) was then added to the residual solids, and insoluble solids (excess $[Mo_6O_{19}][N(C_4H_9)_4]_2$) were removed by filtration. The solvent was evaporated under vacuum again, and the resulting solids were recrystallized twice from acetone/ethyl ether to give 0.32 g of compound **6** (54%, mp: 128−129 °C). ^{1}H NMR (CD_3COCD_3, 250 MHz, 25 °C): δ 7.66 (s, 1H, ArH), 7.53 (d, J = 8.0 Hz, 1H, ArH), 7.45 (d, J = 8.0 Hz, 1H, ArH), 7.26 (s, 2H, ArH), 3.85 (s, 1H, ≡CH), 3.57 (s, 1H, ≡CH), 3.09 (t, J = 7.9 Hz, 16H, NCH_2-), 2.61 (s, 6H, Ar−CH_3), 1.57 (m, 16H, -CH_2-), 1.37 (m, 16H, -CH_2-), 0.96 (t, J = 7.2 Hz, 24H, CH_3). Anal. Calcd for $C_{52}H_{85}Mo_6N_3O_{18}$: C, 38.65; H, 5.30. Found: C, 38.26; H, 5.64. Single crystals suitable for X-ray analysis were grown by slow diffusion of diethyl ether into an acetone solution of **6** at room temperature. A red block-shaped crystal of dimensions 0.50 × 0.27 × 0.25 mm was selected for structural analysis. Summary of crystal structure data for **6**: $C_{52}H_{85}Mo_6N_3O_{18}$, Mr = 1615.87, orthorhombic, $P2_12_12_1$, a = 13.7708(12), b = 17.4272(16), c = 25.724(2) Å, α = 90°, β = 90°, γ = 90°, V = 6173.4(9) Å^3, Z = 4, Z' = 1, T = 100(2) K, 38240 reflections measured, 12098 unique (R_{int} = 0.0270), R_1 = 0.0330, wR_2 = 0.0881, goodness-of-fit 1.053. CCDC-205080 contains the supplementary crystallographic data for this paper. These data can be obtained free of charge via www.ccdc.cam.ac.uk/conts/retrieving.html (or from the Cambridge Crystallographic Data Center).

Compound 7. A mixture containing *p*-methoxyphenol (10 g, 80 mmol), 5-chloro-1-pentyne (8.51 g, 83 mmol), sodium hydroxide (3.54 g, 88.5 mmol), tetrabutylammonium bromide (1.5 g, 4.6 mmol), water (30 mL), and toluene (40 mL) was stirred at 90 °C for 20 h. After being cooled to room temperature, the mixture was poured into water (400 mL) and extracted three times with hexane (3 × 200 mL). The organic layer was collected and dried over $MgSO_4$, and the solvent was then evaporated to yield compound **7** as a colorless oil (14.6 g, 95%). ^{1}H NMR ($CDCl_3$, 400 MHz, 25 °C): δ 1.95−2.01 (m, 3H, -CH_2- and ≡CH), 2.40 (dt, J = 7.2 and 2.8 Hz, 2H, -CH_2-), 3.76 (s, 3H, -OCH_3), 4.01 (t, J = 6.0 Hz, 2H, -OCH_2-), 6.84 (m, 4 H, ArH). ^{13}C NMR ($CDCl_3$, 100 MHz): δ 15.4, 28.5, 55.9, 67.0, 69.0, 83.8, 114.8, 115.7, 153.2, 154.1.

Compound 8. A mixture containing 2,6-diisopropyl-4-iodoaniline (9.76 g, 32.2 mmol), phthalic anhydride (4.8 g, 32.3 mmol), and acetic acid (150 mL) was stirred under reflux for 6 h and was then cooled to room temperature. The product, which precipitated during cooling, was collected by filtration and washed with acetic acid (20 mL) and then with water (3 × 50 mL). It was then dried in a vacuum oven to give 11.7 g of compound **8** as white crystals (84%, mp 269−271 °C). ^{1}H NMR ($CDCl_3$, 400 MHz, 25 °C): δ 1.15 (d, J = 6.80 Hz, 12H, -CH_3), 2.65 (sept. J = 6.80 Hz, 2H, -C*H*$(CH_3)_2$), 7.60 (s, 2H, ArH), 7.80−7.84 (m, 2H, ArH), 7.95−7.99 (m, 2H, ArH). ^{13}C NMR ($CDCl_3$, 100 MHz): δ 23.4, 29.5, 97.3, 124.2, 127.2, 132.0, 133.8, 134.7, 149.9, 168.1.

Compound 9. Compound **7** (3.88 g, 20.4 mmol), compound **8** (8.06 g, 18.6 mmol), bis(triphenylphosphine)palladium (II) chloride (0.25 g, 0.36 mmol), and copper(I) iodide (0.14 g, 0.74 mmol) were added to a 100 mL two-neck flask. The flask was evacuated and backfilled with nitrogen three times. THF (50 mL) and triethylamine (2 mL) were then added to the flask with a syringe. After being stirred at room temperature for 10 h, the reaction mixture was poured into water (400 mL) and extracted with methylene chloride (3 × 200 mL). The organic layer was collected and dried over $MgSO_4$, and the solvent was then evaporated to afford the crude product, which was purified by column chromatography (silica gel, eluent?) to yield compound **9** as white crystals (8.30 g, 90%, mp 137−139 °C). ^{1}H NMR ($CDCl_3$, 400 MHz, 25 °C): δ 1.15 (d, J = 7.20 Hz, 12H, -CH_3), 2.09 (quint, J = 6.40 Hz, 2H, -CH_2-), 2.64−2.69 (m, 4H, -CH_2- and -CH-), 3.78 (s, 3H, -OCH_3), 4.10 (t, J = 6.0 Hz, 2H, -OCH_2-), 6.87 (m, 4H, ArH), 7.30 (s, 2H, ArH), 7.82 (dd, J = 3.2 and 2.4 Hz, 2H, ArH), 7.97 (dd, J = 3.2 and 2.4 Hz, 2H, ArH). ^{13}C NMR ($CDCl_3$, 100 MHz): δ 16.4, 24.0, 28.8, 29.5, 55.9, 67.4, 81.3, 89.9, 114.9, 115.8, 124.1, 125.9, 126.8, 127.6, 132.1, 134.6, 147.6, 153.3, 154.1, 168.2.

Compound 10. Compound **9** (4.5 g, 9.1 mmol), palladium (3% on activated carbon, 300 mg), and acetic acid (50 mL) were added to a three-neck 100 mL flask. The flask was evacuated and backfilled with hydrogen three times. After being stirred under hydrogen (1 atom) for 12 h, the reaction mixture was filtered through Celite 645 (Fisher Co.). The filtrate was poured into water and extracted with methylene chloride (3 × 100 mL). The organic layer was washed with water, dried over $MgSO_4$, and stripped of solvent to afford compound **10** as white solids (4.36 g, 96%, mp 89−90.5 °C). ^{1}H NMR ($CDCl_3$, 400 MHz): δ 1.16 (d, J = 6.80 Hz, 12H, -CH_3), 1.58 (quint, J = 8.0 Hz, 2H, -CH2-), 1.74 (quint, J = 7.7 Hz, 2H, -CH_2-), 1.85 (quint, J = 7.2 Hz, 2H, -CH_2-), 2.69 (t, J = 6.8 Hz, 2H, -CH_2-), 3.77 (s, 3H, -OCH_3), 3.95 (t, J = 6.4 Hz, 2H, -OCH_2-), 6.82−6.87 (m, 4H, ArH), 7.09 (s, 2H, ArH), 7.80−7.84 (m, 2H, ArH), 7.95−7.98 (m, 2H, ArH). ^{13}C NMR ($CDCl_3$, 100 MHz): δ 24.2, 26.3, 29.3, 29.5, 31.3, 36.4, 56.0, 68.8, 114.9, 115.7, 124.0, 124.2, 124.6, 132.2, 134.5, 144.6, 147.1, 153.5, 153.9, 168.6.

Compound 11. A mixture containing compound **10** (5.646 g, 11.3 mmol), iodine (2.83 g, 11.2 mmol), iodic acid (1.25 g, 7.1 mmol), sulfuric acid (10 mL, 30% w/w in H_2O), carbon tetrachloride (10 mL), and acetic acid (40 mL) was stirred under reflux overnight. After being cooled to room temperature, the reaction mixture was poured into methylene chloride (200 mL). The resulting mixture was washed with water (200 mL), aqueous KOH (3 M, 100 mL), and water (200 mL), consecutively. The organic layer was collected and dried over $MgSO_4$, and the solvent was then evaporated to afford the crude product, which was purified by recrystallization from methanol to give compound **11** as white crystals (7.13 g, 84%, mp 182−184 °C). ^{1}H NMR ($CDCl_3$, 400 MHz): δ 1.16 (d, J = 7.20 Hz, 12H, -CH_3), 1.64 (m, 2H, -CH_2-), 1.76 (quint, J = 8.0 Hz, 2H, -CH_2-), 1.88 (quint, J = 7.2 Hz, 2H, -CH_2-), 2.67−2.72 (m, 4H, -CH_2- and -CH-), 3.82 (s, 3H, -OCH_3), 3.97 (t, J = 6.0 Hz, 2H, -OCH_2-), 7.10 (s, 2H, ArH), 7.20 (s, 2H, ArH), 7.81 (dd, J = 3.2 and 2.0 Hz, 2H, ArH), 7.97 (dd, J = 3.2 and 2.0 Hz, 2H, ArH). ^{13}C NMR ($CDCl_3$, 100 MHz): δ 24.2, 26.3, 29.3, 29.5, 31.2, 36.4, 57.4, 70.5, 85.6, 86.7, 121.8, 123.3, 124.0, 124.3, 124.7, 132.2, 134.5, 144.6, 147.2, 153.2, 153.5, 168.6.

Compound 12. The mixture of compound **11** (4.5 g, 6.0 mmol), hydrazine (3 g, 60 mmol), THF (75 mL), and ethanol (75 mL) was refluxed for 48 h. The reaction mixture was cooled to room temperature, followed by the addition of hydrochloric acid (37%, 20 mL). The resulting mixture was refluxed for another 2 h and was then cooled to room temperature. White precipitates were filtered, and the filtrate was poured into water (500 mL). The aqueous solution was extracted with methylene chloride (2 × 300 mL). The organic portions were collected and dried over $MgSO_4$, and the solvent was evaporated. The resulting mixture was subjected to column chromatography (silica gel, hexanes/ethyl acetate (3:1) as the eluent) to give 3.0 g of recovered **11** and the pure compound **12** as pale yellow solids (0.50 g, 40% yield based on reacted **11**, mp 95−97.5 °C). ^{1}H NMR ($CDCl_3$, 400 MHz): δ 1.25 (d, J = 7.2 Hz, 12H, -CH_3), 1.55 (m, 2H, -CH_2-), 1.65 (m, 2H, -CH_2-), 1.83 (quint, J = 7.2 Hz, 2H, -CH_2-), 2.55 (t, J = 7.2 Hz, 2H, -CH_2-), 2.91 (sept, J = 6.8 Hz, 2H, -CH-), 3.60 (s, 2H, NH_2), 3.80 (s, 3H, -OCH_3), 3.92 (t, J = 6.4 Hz, Hz, 2H, -OCH_2-), 6.84 (s, 2H, ArH), 7.17 (s, 2 H, ArH). ^{13}C NMR ($CDCl_3$, 100 MHz): δ 22.8, 26.2,

28.2, 29.3, 31.9, 36.0, 57.4, 70.6, 85.6, 86.7, 121.7, 122.9, 123.3, 132.6, 132.8, 138.2, 153.2, 153.5. Anal. Calcd for $C_{24}H_{33}NO_2I_2$: C, 46.39; H, 5.35. Found: C, 46.62; H, 5.43.

Polymer Ia. A mixture containing compound **5** (0.1000 g, 0.3715 mmol), DCC (0.2297 g, 1.1144 mmol), $[Mo_6O_{19}]$ $[N(C_4H_9)_4]_2$ (2.0267 g, 1.4859 mmol), and CH_3CN (5 mL) was refluxed for 5−7 h, and the solvent was then evaporated under vacuum. To this flask was added monomer **14** (0.5596 g, 1.1144 mmol), bis(triphenylphosphine)palladium (II) chloride (0.0264 g, 0.033 mmol), copper (I) iodide (0.013 g, 0.066 mmol), triethylamine (0.5 mL), THF (5 mL), and DMF (5 mL). The resulting mixture was stirred at room temperature for 30 min, followed by the addition of monomer **15** (0.2217 g, 0.7429 mmol). After being stirred at room temperature for another 12 h, the reaction mixture was filtered through glass wool and was then poured into acetonitrile (250 mL). The yellow precipitates were collected, washed with acetonitrile, and dried in a vacuum to yield polymer **Ia** (0.66 g, 60%). ^{1}H NMR (acetone-d_6, 400 MHz, 25 °C): δ 0.95 (t, J = 7.2 Hz, -CH_3), 1.22 (m and br, C(CH_3)$_3$), 1.44 (br, -CH_2-), 1.78 (br, -CH_2-), 2.86 (br, Ar−CH_3), 3.40 (br, NCH_2-), 3.77 (br, -OCH_2-), 6.82 (br, ArH), 6.95−7.22 (m and br, ArH), 7.36 (br, ArH), 7.47 (br, ArH). Anal. Calcd. for $(C_{140}H_{203}Mo_6N_3O_{28})_n$: C, 56.96; H, 6.93; Mo, 19.50; N, 1.42. Found: C, 56.54; H, 6.52; Mo, 16.07; N, 1.89.

Polymer Ib. Polymer **Ib** was synthesized using the same procedure as that of polymer **Ia** (65%). ^{1}H NMR (acetone-d_6, 400 MHz, 25 °C): δ 0.96 (t, J = 7.2 Hz, -CH_3), 1.22 (m and br, C(CH_3)$_3$), 1.35 (br, -CH_2-), 1.63 (br, -CH_2-), 2.61 (br, Ar−CH_3), 3.31 (br, NCH_2-), 3.65 (br, -OCH_2-), 6.82 (br, ArH), 6.95−7.22 (m and br, ArH), 7.34 (br, ArH). Anal. Calcd for $(C_{212}H_{299}Mo_6N_3O_{36})_n$: C, 63.01; H, 7.46; Mo, 14.24; N, 1.04. Found: C, 64.33; H, 6.38; Mo, 10.30; N, 1.03.

Polymers **IIa** and **IIb** were synthesized using a similar procedure to that of polymer **Ia**, except that the order of adding monomers **14** and **15** was reversed.

Polymer IIa. 67% yield. ^{1}H NMR (acetone-d_6, 400 MHz, 25 °C): δ 0.96 (t, J = 7.4 Hz, -CH_3 of the counterion)m, 1.04−1.19 (m and br, -C(CH_3)$_3$), 1.28 (d, J = 6.4 Hz, -CH(CH_3)$_2$), 1.38−1.48 (m, -CH_2-), 1.63 (br, -CH_2-), 1.70 (br, -CH_2-), 1.76−1.87 (m and br, -CH_2-), 1.89 (br, -CH_2-), 2.52 (br, Ar−CH_2−), 2.70 (br, -CH_2-), 3.42 (t, J = 8.6 Hz, -NCH_2-), 3.75 (br, -OCH_2-), 3.89 (br, OCH_3), 4.10 (br, OCH_2-), 6.79 (br, ArH), 6.95−7.14 (m and br, ArH). Anal. Calcd for $(C_{148}H_{223}Mo_6N_3O_{30})_n$: C, 57.34; H, 7.25; Mo, 18.57; N, 1.36. Found: C, 57.73; H, 6.86; Mo, 15.09; N, 1.21.

Polymer IIb. 61% yield. ^{1}H NMR (acetone-d_6, 400 MHz, 25 °C): δ 0.96 (t, J = 7.4 Hz, -CH_3 of the counterion), 1.04−1.19 (m and br, -C(CH_3)$_3$), 1.28 (d, J = 6.4 Hz, -CH(CH_3)$_2$), 1.38−1.48 (m, -CH_2-), 1.63 (br, -CH_2-), 1.70 (br, -CH_2-), 1.76−1.87 (m and br, -CH_2-), 1.89 (br, -CH_2-), 2.52 (br, Ar−CH_2−), 2.70 (br, -CH_2-), 3.42 (t, J = 8.6 Hz, -NCH_2-), 3.75 (br, -OCH_2-), 3.89 (br, OCH_3), 4.10 (br, OCH_2-), 6.79 (br, ArH), 6.95−7.14 (m and br, ArH). Anal. Calcd for $(C_{220}H_{319}Mo_6N_3O_{38})_n$: C, 63.07; H, 7.67; Mo, 13.74; N, 1.00. Found: C, 60.84; H, 7.06; Mo, 10.40; N, 0.85.

Polymer III. A mixture containing compound **14** (0.3000 g, 0.597 mmol), **15** (0.1783 g, 0.597 mmol), bis(triphenylphosphine)-palladium (II) chloride (0.0168 g, 0.0239 mmol), copper (I) iodide (0.0091 g, 0.0478 mmol), triethylamine (0.4 mL), and DMF (5 mL) was stirred at room temperature for 5 h. The reaction mixture was then filtered through glass wool and then poured into methanol. The polymer precipitates were collected by filtration, washed with methanol, and dried in a vacuum to yield 0.23 g of polymer **III** (72%). ^{1}H NMR ($CDCl_3$, 400 MHz, 25 °C): δ 1.11 (br, C(CH_3)$_3$), 3.65 (br, -OCH_2-), 6.99 (br, ArH). Anal. Calcd for $(C_{18}H_{24}O_2)_n$: C, 79.37; H, 8.88. Found: C, 78.65; H, 8.31.

Acknowledgment. We thank Dr. Douglas R. Powell at the University of Kansas for the X-ray structure determination and Dr. Michelle H. Chen at Wyatt Technologies for the light scattering measurements. This work is supported by the National Science Foundation (DMR 0134032), the Office of Naval Research, and the University of Missouri Research Board.

Supporting Information Available: ^{1}H NMR spectra of compounds **3**−**13** and polymer **IIa**. Data of GPC, light scattering, and viscosity measurements. This material is available free of charge via the Internet at http://pubs.acs.org.

CM050188R